

UNCLASSIFIED

Defense Technical Information Center
Compilation Part Notice

ADP013731

TITLE: Approximation with the Radial Basis Functions of Lewitt

DISTRIBUTION: Approved for public release, distribution unlimited

This paper is part of the following report:

TITLE: Algorithms For Approximation IV. Proceedings of the 2001
International Symposium

To order the complete compilation report, use: ADA412833

The component part is provided here to allow users access to individually authored sections
of proceedings, annals, symposia, etc. However, the component should be considered within
the context of the overall compilation report and not as a stand-alone technical report.

The following component part numbers comprise the compilation report:

ADP013708 thru ADP013761

UNCLASSIFIED

Approximation with the radial basis functions of Lewitt

J. J. Green

Dept. Applied Mathematics, University of Sheffield, UK.

j.j.green@sheffield.ac.uk

Abstract

R. M. Lewitt has introduced a family of compactly supported radial basis functions which are particularly useful in discretising for inversion ill-posed problems involving line integrals. We consider some practical considerations in their use and implementation, compare square and triangular grids of the functions in two dimensions, and describe some particularly favourable choices of the defining parameters.

1 Introduction

In the article [5], R. M. Lewitt introduced a family of window functions

$$\psi(r) = \begin{cases} (1 - (r/a)^2)^{m/2} I_m(\alpha(1 - (r/a)^2)^{1/2}) / I_m(\alpha), & 0 \leq r \leq a, \\ 0, & r > a, \end{cases} \quad (1.1)$$

where I_m is the modified Bessel function of order m (see Ch. III, 3.7 [13]). The implicit dependence of ψ on the parameters $\alpha > 0$, $a > 0$ and $m \in \mathbf{N}$ is discussed below. Lewitt's motivation for studying these functions is the use of translates of the radially symmetric function

$$\Psi(x) = \psi(\|x\|) \quad (x \in \mathbf{R}^d)$$

(see Figure 1) as a basis for the discretisation of tomographic problems [8, 9]. Such a basis overcomes a number of difficulties associated with the usual, pixel-based, representation in problems involving the recovery of function from a set of line, curve or strip integrals across its domain, while retaining the advantage of a *sparse* discretisation. The author's interest in these functions arises in their application to a Radon-like problem in the remote sensing of ocean waves [15], a detailed exposition of which may be found in [3].

2 Discretising x-ray problems

The discretisation of an x-ray transform inversion problem with Lewitt's basis is straightforward. Given a set of *centres* $x_i \in \mathbf{R}^d$, one represents the (unknown) function f as a linear combination of the translates of Ψ ,

$$f(x) = \sum_i \xi_i \Psi(x - x_i) \quad (x \in \mathbf{R}^d). \quad (2.1)$$

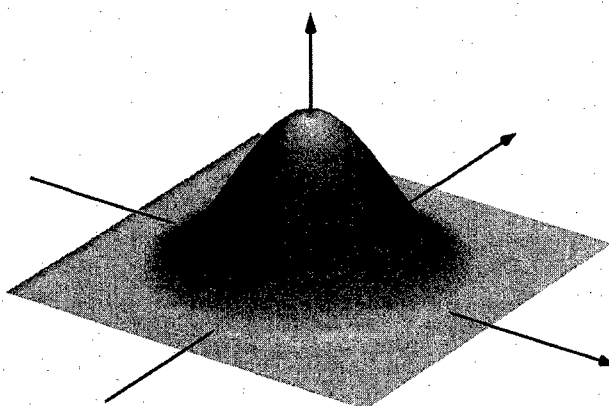


FIG. 1. Lewitt's radial basis function in dimension 2 with $m = 2, \alpha = 3$.

The given data in such problems are the values I_j of integrals of f over lines (or more generally, submanifolds) L_j

$$I_j = \int_{L_j} f(x) = \sum_i \xi_i \int_{L_j} \Psi(x - x_i). \quad (2.2)$$

The latter integral in (2.2) is the *projection* or *Abel transform* of f , which can be calculated explicitly in the linear case. For a line L_j whose closest point to x_i is at a distance s from it, and with the dependence of ψ on m here made explicit,

$$2 \int_0^\infty \psi_m(\sqrt{s^2 + t^2}) dt = a \frac{I_{m+1/2}(\alpha)}{I_m(\alpha)} \left(\frac{2\pi}{\alpha} \right)^{1/2} \psi_{m+1/2}(s)$$

(see A7, [5]). Thus (2.2) reduces to a linear system which may be solved for the coefficients ξ_i . If the support of the basis functions is small (i. e., if a is small) then this linear system has an unstructured sparsity which can be exploited by, for example, an iterative row-action solution method [2].

The computational cost of such a discretisation lies mainly in the evaluation of the Abel transform which requires the calculation of a Bessel function. Fortunately, Bessel functions of half-integer order can be calculated efficiently from their recurrence relations (see the Atlas, [12], for details).

The discretisation techniques described here can also be applied to problems in which the integrals are over curves of sufficient smoothness to allow a local linear approximation.

3 Fourier transform and invertibility

The Fourier transform of the d -dimensional basis function Ψ_m is radially symmetric and given in (A3) of [5] as

$$\hat{\Psi}_m(x) = \frac{a^d \alpha^m (2\pi)^{d/2}}{I_m(\alpha)} \frac{J_{m+d/2}(z)}{z^{m+d/2}}, \quad z = \sqrt{(2\pi a \|x\|)^2 - \alpha^2}. \quad (3.1)$$

The presence of the Bessel function $J_{m+d/2}(z)$ in this expression clearly implies that it is not non-negative, and so by Bochner's characterisation of positive definite translation-invariant functions, Ψ is *not* positive definite for any choices of the parameters.

This fact denies us the attractive approximation theory of the compactly supported radial functions of Wu, Wendland and Buhmann (Section 3, [1]). In particular, there is no guarantee, *per se*, on the invertibility of the interpolation matrix $[\Psi(x_i - x_j)]$, needed to ensure that (2.1) can represent an arbitrary function at its centres. However, this interpolation matrix is invertible if it is strictly diagonally dominant (Corollary 5.6.17, [4]) which, for a set of centres on a uniform grid Γ , holds if

$$\Psi(0) > \sum_{x \in \Gamma \setminus \{0\}} \Psi(x). \quad (3.2)$$

Values of the parameters for which (3.2) is satisfied for the square planar grid $\Delta \mathbf{Z}^2$ are shown in Figure 2.

As is noted in [5], there are several reasons why a rapid decay of the Fourier transform of the basis function is advantageous in functional representation for the inversion of x-ray and related transforms.

- Such inversions may be complicated by functions in the nullspace of the transform, so-called ghosts. For some transforms [7] it can be shown that such functions have a Fourier transform which is small close to zero in the frequency domain, and so representation by a basis with Fourier transform localised around zero will suppress these ghosts.
- These inversions are often *ill-posed* and the given data noisy. Representation of the sought function by a basis with localised Fourier transform imposes smoothness, and so acts to regularise the problem in the sense of Tikhonov.
- It is often convenient to sample the inverted function on a grid which differs from the set of centres x_i of the basis. With a localised Fourier transform, such a sampling can be performed without significant aliasing.

The asymptotic estimate $\hat{\Psi}_m(x) = O(1/\|x\|^{m+(d+1)/2})$ may be derived from (3.1) and estimates I_m with large argument (see Eq. A4, [5]), a fact which should inform our choice of m .

4 Choice of parameters

One agreeable feature of Lewitt's radial functions is that the choice of parameters of the functions correspond in a natural way to the balance between representation quality and efficiency of computation. For example, the asymptotic rate of decay of the Fourier transform increases with m (see above), but so does the cost of the calculation of I_m .

A similar choice arises when the centres lie on a uniform (square or triangular) grid Γ . Let Δ denote the *grid spacing* of such a grid, i. e., the minimum distance between distinct centres in Γ . It is desirable that the *grid ratio* a/Δ be small, as this results in sparsity of the discretisation. As a guide to fixing the values of α and the grid ratio, Lewitt suggests the error in *quasi interpolation to a constant*, the error with which the function

$$g(x) := \sum_{i \in \Gamma} \Psi(x)$$

approximates the function whose constant value is that of g at the centres (edge effects are ignored here). In Figure 2 the root mean square of this representation error (estimated numerically) is shown for the square planar grid, $m = 2$ and a range of values of α and a/Δ . The distinctive "trenches" in the error can be explained with Poisson summation formula (see [11]),

$$\sum_{n \in \mathbf{Z}^2} \Psi(x + \Delta n) = \frac{1}{\Delta^2} \sum_{n \in \mathbf{Z}^2} \exp(2\pi i n \cdot x / \Delta) \hat{\Psi}(n / \Delta). \quad (4.1)$$

The summand for $n = 0$ in the second sum is $\hat{\Psi}(0)$, so the representation error depends only on the values of $\hat{\Psi}$ on the *dual grid*, \mathbf{Z}^2 / Δ . Provided that $\hat{\Psi}$ decays rapidly, we would expect a small error when $\hat{\Psi}$ is zero, or close to zero, for the dual grid-nodes close to the origin.

By (3.1), $\hat{\Psi}(x)$ is zero exactly when

$$J_{m+d/2}(\sqrt{(2\pi a \|x\|)^2 - \alpha^2}) = 0,$$

i. e., for radial values $\|x\| = R_k$,

$$R_k = \frac{1}{2\pi a} \sqrt{\alpha^2 + \eta_k^2} \quad (k = 1, 2, \dots),$$

where η_k is the k -th zero of $J_{m+d/2}$. Thus, the requirement that the k -th zero of $\hat{\Psi}(x)$ occurs at the radius of the closest non-zero dual grid node (i. e., $R_k = 1/\Delta$) is a constraint on the values of α and a/Δ

$$\alpha = \sqrt{(2\pi a / \Delta)^2 - \eta_k^2}. \quad (4.2)$$

The contours (4.2) agree well with the trenches evident in Figure 2. With the same intent we can require that the l -th zero of $\hat{\Psi}(x)$ occur at the radius of the *second* closest dual grid node ($R_l = \sqrt{2}/\Delta$). Points satisfying *both* of these constraints can be expected to have a particularly small representation error. In Figure 2 these favourable choices are labelled **k:1**.

The above argument can be also be applied the triangular grid. Establishing the Poisson summation formula for such is straightforward (either generalised from VII Section 2 of [11] or specialised from the formula for topological groups in [6]), and one finds that dual grid is the triangular grid with node spacing $2/(\Delta\sqrt{3})$. The representation error is, qualitatively, similar to that shown in Figure 2. To make a quantitative comparison we plot, in Figure 3, the representation error on the principal trench (i. e., along the contour

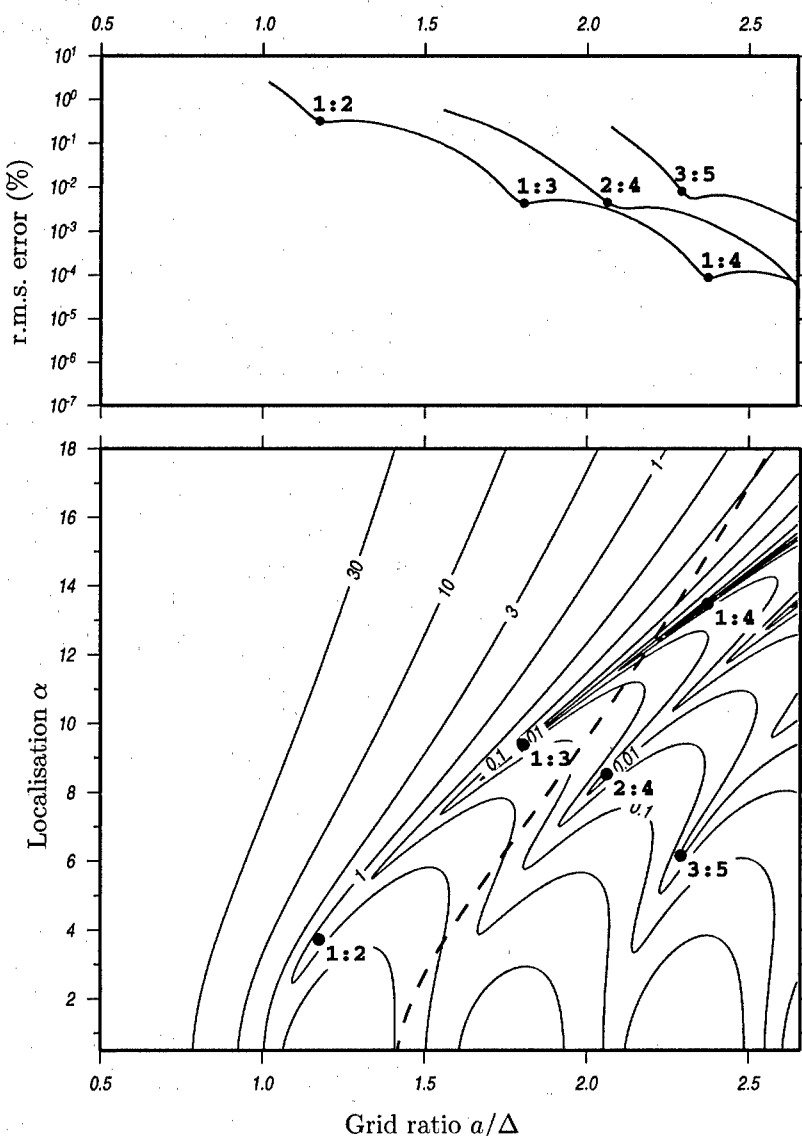


FIG. 2. The representation error of the square planar grid for $m = 2$. The lower contour map shows the root mean square error in representation for different values of the grid ratio a/Δ and localisation α . The upper figure shows the error along the trenches evident in the lower. Favourable choices of the parameters are marked $1:2, 1:3, \dots$, and are also shown in the lower figure. Values of the parameters to the left of the dashed line give rise to a diagonally dominant interpolation matrix.

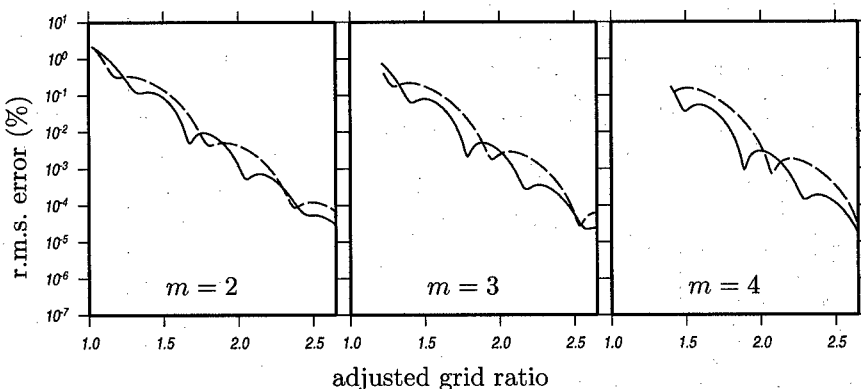


FIG. 3. Error in the principal trench for square (dashed) and triangular (solid) grids.

(4.2) for $k = 1$ in the case of the square grid) for each grid type and a number of values of m .

To ensure a fair comparison, the horizontal scale in Figure 3 is adjusted for each grid-type to give equal node densities. As is seen, the two grid-types have similar error performance, suggesting that the square grid (with attendant ease of implementation) is to be preferred in practice.

5 The functions of Wendland

It is interesting to compare Lewitt's functions with the radial basis functions of Wendland [1, 14], positive definite functions whose window functions are piecewise polynomial. The positive definiteness of Wendland's functions indicate their usefulness in approximation, for which extensive results exist, and a number of recent papers have explored their use in the discretisation of partial differential equations.

The use of Wendland's functions in x-ray problems does not appear to have been investigated, although their Abel transforms can be obtained analytically. We do not address this question here, but indicate why Lewitt's functions *may* offer some advantages for such problems. The Fourier transform of Wendland's function $\Phi_{2,0}$, whose window is $\phi_{2,0}(r) = (1 - r)_+^2$, is proportional to

$$r^{-4} \int_0^{2\pi r} (2\pi r - t)^2 t J_0(t) dt = O(r^{-3}) \quad (r = \|x\|)$$

(see Section 3, [14]). In Figure 4, $\hat{\Phi}_{2,0}$ is plotted along with the Fourier transform $\hat{\Psi}_2$, of Lewitt's function with $a = 1$ and the parameter choice 1:2 of Figure 2. Although both have the same *asymptotic* decay of the Fourier transform, Lewitt's is more localised about zero and thus *may* offer better suppression of ghosts in x-ray problems.

Finally we mention that Buhmann has shown, in [1], that Wendland's window func-

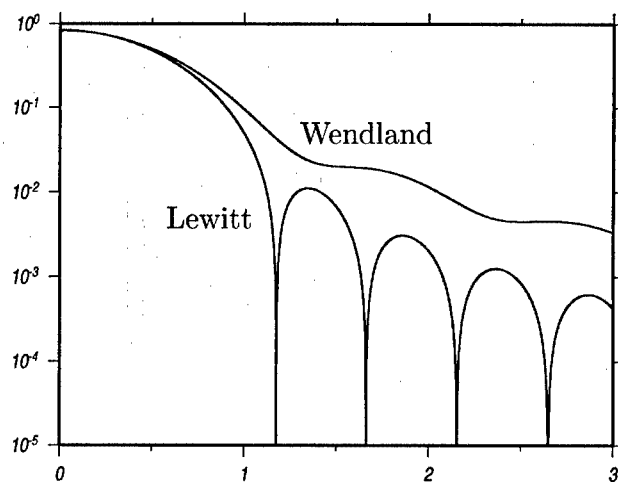


FIG. 4. Fourier transforms of basis functions.

tion admits a convolution representation of the form

$$\rho(r) := \int_0^\infty (1 - r^2/t)_+^n t^n g(t) dt \quad (5.1)$$

for the weight $g(t) = (1 - t)_+^k$ with suitable k and n . We note that (5.1) may be solved for g , since substituting $x = r^2$ in (5.1) allows it to be reduced to a standard integral equation whose solution,

$$g(x) = \frac{(-1)^n}{n!} f^{(n)}(x), \quad f(x) = \rho(r),$$

can be found in Article 1.1–4.32 of [10]. In the case that ρ is Lewitt's window ψ_m , one may use the differentiation formula, A11 of [5], to find the corresponding weight g . For $n = 1$ we find that

$$g(x) = -\frac{1}{2\alpha^{m-2}} \frac{I_{m-1}(\alpha)}{I_m(\alpha)} \psi_{m-1}(r),$$

a weight qualitatively different from that of Wendland's function.

Acknowledgements: The author wishes to thank L. R. Wyatt and the referees for a number of helpful comments, and acknowledges the financial support provided by the EC with the grant MAS3-CT98-0168.

Bibliography

1. M. D. Buhmann. Radial basis functions. In *Acta Numerica*, volume 9, pages 1–38. Cambridge University Press, 2000.
2. Y. Censor. Row-action methods for huge and sparse systems and their applications. *SIAM Review*, 23(4):444–466, October 1981.
3. J. J. Green. Discretizing Barrick's equations. Submitted.

4. R. A. Horn and C. R. Johnson. *Matrix Analysis*. Cambridge University Press, 1990.
5. R. M. Lewitt. Multidimensional digital image representations using generalized Kaiser-Bessel window functions. *J. Opt. Soc. Am. A*, 7(10):1834–1846, October 1990.
6. L. H. Loomis. *An Introduction to Abstract Harmonic Analysis*. D. Van Nostrand, 1953.
7. A. K. Louis. Orthogonal function series expansion and the null space of the Radon transform. *SIAM J. Math. Anal.*, 15(3):621–633, May 1984.
8. S. Matej, G. T. Herman, T. K. Narayan, S. S. Furuie, R. M. Lewitt, and P. E. Kinahan. Evaluation of task-oriented performance of several fully 3d PET reconstruction algorithms. *Phys. Med. Biol.*, 39:355–367, 1994.
9. S. Matej and R. M. Lewitt. Practical considerations for 3-d image reconstructions using spherically symmetric volume elements. *IEEE Transactions on Medical Imaging*, 15(1):68–78, 1996.
10. A. D. Polianin and V. Manzhirov. *Handbook of Integral Equations*. CRC Press, 1998.
11. E. M. Stein and G. Weiss. *Fourier Analysis on Euclidean Spaces*. Princeton University Press, 1971.
12. William J. Thompson. *Atlas for computing mathematical functions*. John Wiley & Sons Inc., New York, 1997.
13. G. N. Watson. *A Treatise on the Theory of Bessel Functions*. Cambridge, second edition, 1944.
14. H. Wendland. Error estimates for interpolation by compactly supported radial basis functions of minimal degree. *Journal of Approximation Theory*, 93:258–272, 1998.
15. L. R. Wyatt. A relaxation method for integral inversion applied to HF radar measurement of the ocean wave directional spectrum. *International J. Remote Sensing*, 11:1481–1494, 1990.